Syntheses and Reactivity of Ruthenium σ-Pyridylacetylides

Iuan-Yuan Wu,† Jiann T. Lin,*,† Jimmy Luo,‡ Shih-Sheng Sun,† Chyi-Shiun Li,† Kuan J. Lin,† Chiitang Tsai,‡ Chia-Chen Hsu,§ and Jiunn-Lih Lin§

Institute of Chemistry, Academia Sinica, Nankang, Taipei, Taiwan, Republic of China, Department of Chemistry, Chinese Culture University, Taipei, Taiwan, Republic of China, and Department of Physics, National Chung Cheng University, Ming-Hsiung, Chia-Yi, Taiwan, Republic of China

Received December 17, 1996⊗

Ruthenium σ-acetylides containing a dangling pyridine were synthesized from the reactions of $CpRu(L)_2Cl$ (L = PPh_3, $^1/_2$ $(C_5H_4PPh_2)_2Fe$) with 4-ethynylpyridine, (*E*)-1-(4-ethynylphenyl)-2-(4-pyridyl)ethylene, or 4-(ethynylphenyl)(4-pyridyl)acetylene in the presence of $NH_4^+PF_6^-$ followed by deprotonation with a base. The dangling pyridine can be protonated, methylated, or ligated to tungsten carbonyl fragments. The ruthenium donor to the pyridinium acceptor charge-transfer absorption appears at longer wavelength as the conjugation chain becomes longer. The quadratic hyperpolarizabilities of the methylated derivatives were determined using the hyper Rayleigh scattering method. X-ray analysis was employed to examine the structure of the dinuclear complex $Ru(C{\equiv}CC_5H_4N\{W(CO)_4(PPh_3)\})(\eta^2\text{-dppf})(\eta^5\text{-}C_5H_5)$ (dppf = 1,1′-bis(diphenylphosphino)ferrocene).

Introduction

Metal acetylides are invloved in several important organometallic processes such as surface organometallics and palladium catalyzed carbon-carbon coupling reactions.[1] Metal acetylides have also attracted considerable study due to their possible applications in materials chemistry.[2] The pioneering work by Green and co-workers on organometallic nonlinear optics[3] has stimulated considerable effort in this area.[4] Metal σ-acetylide complexes are potentially useful nonlinear optical materials, since the metal atom resides in the same plane as the π-system, a criterion suggested by Marder.[5] Cyclopentadienylruthenium σ-acetylides are of interest because of their easy preparation.[6] In addition, the electron-donating capability of the ruthenium moiety has been found to be beneficial to molecular quadratic hyperpolarizability.[7] Systematic studies of these ruthenium complexes on optical nonlinearity have also appeared recently.[8]

We have been interested in transition-metal complexes ligated with conjugated pyridines[9] for applications in materials chemistry. In view of the fact that the pyridine ring can function as an electron acceptor upon coordination to an organometallic electron acceptor moiety,[10] we set out to assemble a cyclopentadienylruthenium σ-acetylide donor and a pyridylmetal group in the same molecule. Here we report the syntheses and characterization of such dinuclear complexes. Some mononuclear ruthenium σ-acetylides with a pyridinium acceptor are also included.

Experimental Section

The general procedures and physical measurements are those described in an earlier report.[9] 4-Ethynylpyridine,[11] $RuCl(PPh_3)_2(\eta^5\text{-}C_5H_5)$,[12] $RuCl(\eta^2\text{-dppf})(\eta^5\text{-}C_5H_5)$ (dppf = 1,1′-bis(diphenylphosphino)ferrocene),[13] $W(CO)_5L$ (L = PPh_3, PMe_3),[14] $W(CO)_3$(dppe)(acetone),[15] and $[(MeCN)Re(2,2'\text{-bpy})(CO)_3][PF_6]$[16] were prepared by following the published methods.

$[Ru(C{\equiv}CC_5H_4NH)(PPh_3)_2(\eta^5\text{-}C_5H_5)][PF_6]$ (1). A solution of 4-ethynylpyridine (340 mg, 2.75 mmol) in MeOH (50 mL) was added to a solution of $RuCl(PPh_3)_2(\eta^5\text{-}C_5H_5)$ (2.0 g, 2.75 mmol) and $NH_4^+PF_6^-$ (540 mg, 3.31 mmol) in 100 mL of CH_2-

* To whom correspondence should be addressed. Telefax: 886-2-7831237. E-mail: jtlin@chem.sinica.edu.tw.
† Academia Sinica.
‡ Chinese Culture University.
§ National Chung Cheng University.
⊗ Abstract published in *Advance ACS Abstracts*, April 15, 1997.

(1) (a) Beck, W.; Niemer, B.; Wieser, M. *Angew. Chem., Int. Ed. Engl.* **1993**, *32*, 923. (b) Hegedus, L. S. In *Organometallics in Synthesis*; Schlosser, M., Ed.; Wiley: New York, 1994; p 383.
(2) (a) Myers, L. K.; Langhoff, C.; Thompson, M. E. *J. Am. Chem. Soc.* **1992**, *114*, 7560. (b) Kaharu, T.; Matsubara, H.; Takahashi, S. *J. Mater. Chem.* **1992**, *2*, 43. (c) Hagihara, M.; Sonogashira, K.; Takahashi, S. *Adv. Polym. Sci.* **1981**, *41*, 149.
(3) Green, M. L. H.; Marder, S. R.; Thompson, M. E.; Bandy, J. A.; Bloor, D.; Kolinsky, P. V.; Jones, K. J. *Nature (London)* **1987**, *330*, 360.
(4) (a) Long, N. J. *Angew. Chem.. Int. Ed. Engl.* **1995**, *34*, 21. (b) Kanis, D. R.; Ratner, M. A.; Marks, T. J. *J. Am. Chem. Soc.* **1992**, *114*, 10338.
(5) Calabrese, J. C.; Cheng, L. T.; Green, J. C.; Marder, S. R.; Tam, W. *J. Am. Chem. Soc.* **1992**, *113*, 7227.
(6) Davies, S. G.; McNally, J. P.; Smallridge, A. J. In *Advances in Organometallic Chemistry*; West, R., Stone, F. G. A., Eds.; Academic: New York, 1990; Vol. 30, p 30.
(7) Laidlaw, W. M.; Denning, R. G.; Verbiest, T.; Chauchard, E.; Persoons, A. *Nature (London)* **1993**, *363*, 58.
(8) (a) Whittall, I. R.; Humphrey, M. G.; Hockless, D. C. R.; Skelton, B. W.; White, A. H. *Organometallics* **1995**, *14*, 3970. (b) Whittall, I. R.; Humphrey, M. G.; Persoons, A.; Houbrechts, S. *Organometallics* **1996**, *15*, 1935.
(9) (a) Lin, J. T.; Sun, S. S.; Wu, J. J.; Lee, L. S.; Lin, K. J.; Huang, Y. F. *Inorg. Chem.* **1995**, *34*, 2323. (b) Lin, J. T.; Sun, S. S.; Wu, J. J.; Liaw, Y. C.; Lin, K. J. *J. Organomet. Chem.* **1996**, *517*, 217.
(10) (a) Kanis, D. R.; Lacroix, P. G.; Ratner, M. A.; Marks, T. J. *J. Am. Chem. Soc.* **1994**, *116*, 10089. (b) Bourgault, M.; Mountassir, C.; Le Bozec, H.; Ledoux, I.; Pucetti, G.; Zyss, J. *J. Chem. Soc., Chem. Commun.* **1993**, 1623.
(11) King, R. B., Ed. *Organometallic Synthesis, Transition-Metal Compounds*; Academic: New York, 1965; Vol. 1.
(12) Bruce, M. I.; Hameister, C.; Swincer, A. G.; Wallis, R. C. *Inorg. Synth.* **1990**, *28*, 270.
(13) Sato, M.; Sekino, M. *J. Organomet. Chem.* **1993**, *444*, 185.
(14) (a) Kolodziej, R. M.; Lees, A. J. *Organometallics* **1986**, *5*, 450. (b) Bancroft, R. T.; Arndt, L. W.; Delord, T.; Darensbourg, M. Y. *J. Am. Chem. Soc.* **1986**, *108*, 2617.
(15) Birdwhistell, K. R. *Inorg. Synth.* **1992**, *29*, 141.
(16) Caspar, J. V.; Meyer, T. J. *J. Phys. Chem.* **1983**, *87*, 952.

S0276-7333(96)01065-5 CCC: $14.00

Cl_2. The mixture was stirred at room temperature for 20 h. The solution was then pumped dry and the residue recrystallized from CH_2Cl_2/hexane to provide brownish **1** in 63% yield (1.64 g). Anal. Calcd for $C_{48}H_{40}F_6NP_3Ru$: C, 61.02; H, 4.27; N, 1.49. Found: C, 61.14; H, 4.08; N, 1.32.

[Ru(C≡CC$_5$H$_4$NH)(η^2-dppf)(η^5-C$_5$H$_5$)][PF$_6$] (2). Complex **2** was synthesized by the same procedure employed for **1**, except that RuCl(η^2-dppf)(η^5-C_5H_5) was used instead of RuCl(PPh_3)$_2$(η^5-C_5H_5). The brownish complex **2** was isolated in 87% yield. Anal. Calcd for $C_{46}H_{38}F_6NP_3FeRu$: C, 57.04; H, 3.93; N, 1.45. Found: C, 57.20; H, 4.27; N, 1.40.

(*E*)-1-(4-Bromophenyl)-2-(4-pyridyl)ethylene (3). A pressure tube was charged with 1-bromo-4-iodobenzene (5.66 g, 20.0 mmol), $Pd(OAc)_2$ (45 mg, 0.20 mmol), NEt_3 (6 mL), CH_3CN (4 mL), and 4-vinylpyridine (2.39 mL, 22.0 mmol) under a nitrogen atmosphere. The mixture was heated to 100−110 °C for 36 h; when it was cooled to room temperature, aggregation occurred to form a solid. It was then extracted with a mixture of CH_2Cl_2/H_2O. The organic layer was collected, dried over $MgSO_4$, passed through a neutral alumina column (2 cm in length), and dried. The crude product was recrystallized from CH_2Cl_2/hexane to afford **3** as a white powder (4.67 g, 90%); mp 157.0−157.5 °C. ^1H NMR ($CDCl_3$): δ 8.56 (d, 2 H, J_{H-H} = 6.1 Hz, NC*H*), 7.49 (d, 2 H, J_{H-H} = 8.4 Hz, C_6H_4), 7.38 (d, 2 H, C_6H_4), 7.33 (d, 2 H, NCHC*H*), 7.20 (d, 2 H, J_{H-H} = 16.4 Hz, =C*H*), 6.98 (d, 2 H, =C*H*). Anal. Calcd for $C_{13}H_{10}BrN$: C, 60.02; H, 3.88; N, 5.38. Found: C, 60.02; H, 4.09; N, 5.38.

4-[4-(2-(4-Pyridyl-(*E*)-ethenyl)phenyl]-2-methyl-3-butyn-2-ol (4). To a flask containing a mixture of **3** (5.20 g, 20.0 mmol), $PdCl_2(PPh_3)_2$ (140 mg, 0.24 mmol), CuI (46 mg, 0.24 mmol), and Et_2NH (70 mL) was added 2-methyl-3-butyn-2-ol (2.30 mL, 24.0 mmol). The resulting mixture was refluxed for 20 h to afford an orange-yellow slurry. The slurry was pumped dry, and the residue was extracted with CH_2Cl_2/H_2O. The organic layer was collected, dried over $MgSO_4$, passed through a neutral alumina column (2 cm in length), and dried. The crude product was washed with hexane (2 × 10 mL) to afford **4** as a white powder (4.00 g, 76%). ^1H NMR ($CDCl_3$): δ 8.58 (br, 2 H, NC*H*), 7.46 (d, 2 H, J_{H-H} = 8.3 Hz, C_6H_4), 7.42 (d, 2 H, C_6H_4), 7.35 (d, 2 H, J_{H-H} = 6.1 Hz, NCHC*H*), 7.25 (d, 2 H, J_{H-H} = 16.3 Hz, =C*H*), 7.01 (d, 2 H, =C*H*), 1.61 (s, 6 H, C*H*$_3$). The compound was not purified and was adequate for further reaction.

(*E*)-1-(4-Ethynylphenyl)-2-(4-pyridyl)ethylene (5). Approximately 50 mL of benzene was added to a flask containing **4** (2.50 g, 9.5 mmol) and powdery KOH (0.50 g, 8.9 mmol). The mixture was stirred for 16 h, cooled, filtered through Celite, and dried. Recrystallization of the crude product from CH_2Cl_2/hexane provides white powdery **5** in 79% yield (1.55 g). mp 205.0−205.5 °C. MS (EI): *m/e* 205 (M^+). Anal. Calcd for $C_{15}H_{11}N$: C, 87.77; H, 5.40; N, 6.82. Found: C, 87.57; H, 5.50; N, 6.73.

[Ru(C≡CC$_6$H$_4$CH=CHC$_5$H$_4$NH)(PPh$_3$)$_2$(η^5-C$_5$H$_5$)][PF$_6$] (6a) and [Ru(=C=C(H)C$_6$H$_4$CH=CHC$_5$H$_4$N)(PPh$_3$)$_2$(η^5-C$_5$H$_5$)][PF$_6$] (6b). To a mixture of RuCl(PPh_3)$_2$(η^5-C_5H_5) (1.45 g, 2.00 mmol), $NH_4^+PF_6^-$ (360 mg, 2.20 mmol), and **5** (490 mg, 2.40 mmol) was added 50 mL of CH_2Cl_2 and 10 mL of MeOH. The resulting mixture was stirred at room temperature for 16 h. The solvent was removed under vacuum, and the residue was extracted with CH_2Cl_2 (30 mL). The CH_2Cl_2 solution was filtered through Celite and the filtrate added dropwise to a rapidly stirred mixture of Et_2O (200 mL) and hexane (200 mL). The solution was filtered, and the filtrate was pumped dry. The yellow residue was dissolved in 25 mL of CH_2Cl_2/hexane (1:10) and refrigerated for 2 days to provide an orange-yellow crystalline material which contains **6a** and **6b** (1.67 g, 80%). Anal. Calcd for $C_{56}H_{46}F_6NP_3Ru$: C, 64.61; H, 4.45; N, 1.35. Found: C, 64.08; H, 4.65; N, 1.30. Complex **9** (vide infra) was also isolated from the Et_2O washings in 17% yield (310 mg).

Ru(C≡CC$_5$H$_4$N)(PPh$_3$)$_2$(η^5-C$_5$H$_5$) (7). To a THF solution (50 mL) of **1** (1.00 g, 1.06 mmol) was added dropwise 1,8-diazabicyclo[5.4.0]undec-7-ene (DBU; 1.91 mL, 1.28 mmol). The solution was stirred for 1 h at room temperature and the solvent removed under vacuum. The residue was chromatographed under nitrogen. Elution by CH_2Cl_2/hexane (1:10) provided a yellow band from which a powdery **7** was isolated in 52% yield (437 mg). Anal. Calcd for $C_{48}H_{39}NP_2Ru$: C, 72.72; H, 4.96; N, 1.77. Found: C, 72.55; H, 5.20; N, 1.69.

Ru(C≡CC$_5$H$_4$N)(η^2-dppf)(η^5-C$_5$H$_5$) (8). Complex **8** was synthesized by the same procedure as for the synthesis of **7**, except that **2** was used instead of **1**. The orange-red **8** was isolated in 65% yield. Anal. Calcd for $C_{46}H_{37}NP_2FeRu$: C, 67.16; H, 4.53; N, 1.70. Found: C, 66.88; H, 4.71; N, 1.55.

Ru(C≡CC$_6$H$_4$CH=CHC$_5$H$_4$N)(PPh$_3$)$_2$(η^5-C$_5$H$_5$) (9). An orange-yellow precipitate rapidly formed upon addition of a MeOH solution of NaOMe (0.10 M, 15 mL) to a solution of **6** (1.04 g, 1.00 mmol) in MeOH (60 mL) over a period of 10 min. The solution was stirred for a further 15 min, and 300 mL of H_2O was added to cause a complete precipitation of the product. The precipitate was collected on a fritted-glass filter, and then washed five times with 30 mL of H_2O. The crude product was recrystallized from CH_2Cl_2/hexane to afford orange-yellow crystalline **9** in 89% yield (800 mg). Anal. Calcd for $C_{56}H_{45}NP_2Ru$: C, 75.15; H, 5.07; N, 1.57. Found: C, 74.66; H, 5.31; N, 1.61.

(4-Bromophenyl)(4-pyridyl)acetylene (10). A flask was charged with 4-ethynylpyridine (1.03 g, 10.0 mmol), 1-bromo-4-iodobenzene (2.83 g, 10.0 mmol), $PdCl_2(PPh_3)_2$ (70 mg, 0.12 mmol), CuI (23 mg, 0.12 mmol), and 40 mL of Et_2NH was added to it. The mixture was then stirred at room temperature for 16 h. The solvent was removed under vacuum, and the yellow residue was extracted with CH_2Cl_2/H_2O. The organic layer was collected, dried over $MgSO_4$, passed through a neutral alumina column (2 cm in length), and dried. The crude product was further washed with hexane (2 × 10 mL) to give **10** as a pale yellow powder (2.28 g, 88%); mp 142.5−143.0 °C. ^1H NMR ($CDCl_3$): δ 8.58 (d, 2 H, J_{H-H} = 6.1 Hz, NC*H*), 7.49 (d, 2 H, J_{H-H} = 8.6 Hz, C_6H_4), 7.39 (d, 2 H, C_6H_4), 7.35 (d, 2 H, NCHC*H*). Anal. Calcd for $C_{13}H_8BrN$: C, 60.49; H, 3.12; N, 5.43. Found: C, 60.58; H, 3.27; N, 5.36.

[4-(Trimethylsilyl)ethynyl](4-pyridyl)acetylene (11). (Trimethylsilyl)acetylene (1.42 mL, 10.0 mmol) was added to a flask containing **10** (2.06 g, 8.0 mmol), $PdCl_2(PPh_3)_2$ (120 mg, 0.20 mmol), CuI (19 mg, 0.10 mmol), and Et_2NH (40 mL). The resulting mixture was heated to 40 °C for 16 h. The solvent was removed under vacuum, and the residue was extracted with CH_2Cl_2/H_2O. The organic layer was collected, dried over $MgSO_4$, passed through a neutral alumina column (2 cm in length), and dried. The crude product was further washed with hexane (2 × 10 mL) to give **11** as a white powder (1.72 g, 78%). ^1H NMR ($CDCl_3$): δ 8.56 (d, 2 H, J_{H-H} = 6.0 Hz, NC*H*), 7.43 (s, 4 H, C_6H_4), 7.33 (d, 2 H, NCHC*H*), 0.23 (s, 9 H, C*H*$_3$). The compound was not purified and was adequate for further reaction.

(4-Ethynylphenyl)(4-pyridyl)acetylene (12). Powdery KOH (168 mg, 3.0 mmol) was added to a solution of **11** (826 mg, 3.0 mmol) in 40 mL of MeOH, and the resulting solution was stirred at room temperature for 2 h. The solvent was removed under vacuum, and the residue was extracted with CH_2Cl_2/H_2O. The organic layer was collected, dried over $MgSO_4$, filtered, and dried. The yellow-brown powder was chromatographed using CH_2Cl_2/hexane (1:1) as eluent to afford **12** as a white powder in 92% yield (560 mg); mp 179.5−180.0 °C. MS (EI): *m/e* 203 (M^+). Anal. Calcd for $C_{15}H_9N$: C, 88.64; H, 4.46; N, 6.89. Found: C, 88.66; H, 4.54; N, 6.71.

[Ru(C≡CC$_6$H$_4$C≡CC$_5$H$_4$NH)(PPh$_3$)$_2$(η^5-C$_5$H$_5$)][PF$_6$] (13a) and [Ru(=C=C(H)C$_6$H$_4$C≡CC$_5$H$_4$N)(PPh$_3$)$_2$(η^5-C$_5$H$_5$)][PF$_6$] (13b). A mixture of complexes **13a** and **13b** was synthesized in a manner similar to that employed for **9**, except that **12** was used instead of **6**. The dark brown complex **13** was isolated in 70% yield. Complex **14** (vide infra) was also isolated in 23% yield from the Et_2O washings. MS (FAB): *m/e* 896 ($M^+ - PF_6$). Anal. Calcd for $C_{56}H_{44}F_6NP_3Ru$: C, 64.37; H, 4.24; N, 1.34. Found: C, 64.18; H, 4.71; N, 1.25.

Ru(C≡CC$_6$H$_4$C≡CC$_5$H$_4$N)(PPh$_3$)$_2$(η^5-C$_5$H$_5$) (14). Complex **14** was synthesized by the same procedure employed for **9**, except that **13** was used instead of **6**. The yellow complex **14** was isolated in 92% yield (820 mg). MS (FAB): *m/e* 895 (M$^+$). Anal. Calcd for $C_{56}H_{43}NP_2Ru$: C, 75.32; H, 4.85; N, 1.57. Found: C, 74.76; H, 5.20; N, 1.58.

Ru(C≡CC$_5$H$_4$N{W(CO)$_4$L})(PPh$_3$)$_2$(η^5-C$_5$H$_5$) (15, L = CO; 16, L = PPh$_3$; 17, L = PMe$_3$). Essentially the same procedures were applied to synthesize **15**−**17**; consequently, only the preparation of **17** is described in detail. A THF solution of W(CO)$_4$(PMe$_3$)(THF)[14] prepared in situ from W(CO)$_5$(PMe$_3$) (600 mg, 1.51 mmol) was reduced in volume and transferred to a flask containing **7** (1.00 g, 1.26 mmol). The solution was stirred at room temperature for 20 h and the solvent removed under vacuum. The residue was chromatographed in nitrogen. Elution by CH$_2$Cl$_2$/hexane (1:5) caused a yellow band to appear from which yellow powdery **17** was isolated in 41% yield (602 mg). Anal. Calcd for $C_{55}H_{48}NO_4P_3RuW$: C, 56.71; H, 4.15; N, 1.20. Found: C, 56.41; H, 4.38; N, 1.04.

The yellow complex **15** was isolated with a yield of 36%. Anal. Calcd for $C_{53}H_{39}NO_5P_2RuW$: C, 57.00; H, 3.52; N, 1.25. Found: C, 56.65; H, 3.38; N, 1.12.

The yellow complex **16** was isolated with a yield of 32%. Anal. Calcd for $C_{70}H_{54}NO_4P_3RuW$: C, 62.23; H, 4.03; N, 1.04. Found: C, 62.06; H, 4.09; N, 0.86.

Ru(C≡CC$_5$H$_4$N{W(CO)$_4$L})(η^2-dppf)(η^5-C$_5$H$_5$) (18, L = CO; 19, L = PPh$_3$; 20, L = PMe$_3$). Complexes **18**−**20** were synthesized in a manner similar to that employed for **15**−**17**, except that RuCl(η^2-dppf)(η^5-C$_5$H$_5$) was used instead of RuCl(PPh$_3$)$_2$(η^5-C$_5$H$_5$). The yellow complex **18** was isolated in 39% yield. Anal. Calcd for $C_{51}H_{37}NO_5P_2FeRuW$: C, 53.42; H, 3.25; N, 1.22. Found: C, 53.09; H, 3.21; N, 1.27.

The yellow complex **19** was isolated with a yield of 41%. Anal. Calcd for $C_{68}H_{52}NO_4P_3FeRuW$: C, 59.15; H, 3.80; N, 1.01. Found: C, 58.83; H, 4.00; N, 0.93.

The yellow complex **20** was isolated with a yield of 35%. Anal. Calcd for $C_{53}H_{46}NO_4P_3FeRuW$: C, 53.29; H, 3.88; N, 1.17. Found: C, 52.92; H, 3.68; N, 1.06.

Ru(C≡CC$_5$H$_4$N{W(CO)$_3$(dppe)})(PPh$_3$)$_2$(η^5-C$_5$H$_5$) (21). A THF solution (50 mL) of W(CO)$_3$(dppe)(acetone) (360 mg, 0.50 mmol) was added slowly to a solution of **7** (400 mg, 0.50 mmol) in THF (50 mL). The solution was stirred at room temperature for 2 h and filtered through Celite. After removal of the solvent, the residue was dissolved in CH$_2$Cl$_2$/hexane (1:5); this solution was stored at 0 °C for 2 days. The yellow precipitate formed was collected on a fritted-glass filter, washed two times with 10 mL of hexane, and pumped dry to provide **21** in 81% yield (590 mg). Anal. Calcd for $C_{77}H_{63}NO_3P_4RuW$: C, 63.38; H, 4.35; N, 0.96. Found: C, 62.07; H, 4.41; N, 0.84.

Ru(C≡CC$_6$H$_4$CH=CHC$_5$H$_4$N{W(CO)$_3$(dppe)})(PPh$_3$)$_2$(η^5-C$_5$H$_5$) (22). Complex **22** was synthesized by the same procedures as for the synthesis of **21**, except that **9** was used instead of **7**. Yellow powdery **22** was isolated in 80% yield. Anal. Calcd for $C_{85}H_{69}NO_3P_4RuW$: C, 65.39; H, 4.45; N, 0.90. Found: C, 65.19; H, 4.61; N, 0.86.

[Re(NC$_5$H$_4$C≡CH)(2,2′-bpy)(CO)$_3$][PF$_6$] (23). Freshly distilled THF (150 mL) was transferred to a flask containing a mixture of [(MeCN)Re(2,2′-bpy)(CO)$_3$][PF$_6$] (835 mg, 1.38 mmol) and 4-ethynylpyridine (150 mg, 1.46 mmol). The mixture was refluxed in the dark for 5 h. The solvent was then removed under vacuum and the residue obtained was washed several times with Et$_2$O to give yellow powdery **23** in 73% yield (680 mg). Anal. Calcd for $C_{20}H_{13}F_6N_3O_3PRe$: C, 35.30; H, 1.93; N, 6.18. Found: C, 35.05; H, 1.92; N, 6.09.

[Ru(=C=C(H)C$_5$H$_4$N{Re(CO)$_3$(2,2′-bpy)})(PPh$_3$)$_2$(η^5-C$_5$H$_5$)][PF$_6$]$_2$ (24). The synthesis of **24** is analogous to the synthesis of **1**, except that **23** was used instead of 4-ethynylpyridine. Orange powdery **24** was isolated in 60% yield. Anal. Calcd for $C_{61}H_{48}F_{12}N_3O_3P_4ReRu$: C, 48.13; H, 3.18; N, 2.76. Found: C, 47.90; H, 2.92; N, 2.75.

[Ru(C≡CC$_5$H$_4$N{Re(CO)$_3$(2,2′-bpy)})(PPh$_3$)$_2$(η^5-C$_5$H$_5$)][PF$_6$] (25). Complex **24** (75 mg, 0.050 mmol) was dissolved in CH$_2$Cl$_2$ (15 mL), and 5 mL of NEt$_3$ was added. The mixture was stirred for 3 h, and the solvent was removed under vacuum. The residue was then recrystallized from CH$_2$Cl$_2$/hexane. The crude product was further washed with Et$_2$O and hexane to afford yellow powdery **25** in 59% yield (40 mg). Anal. Calcd for $C_{61}H_{47}F_6N_3O_3P_3ReRu$: C, 53.47; H, 3.46; N, 3.07. Found: C, 53.22; H, 3.30; N, 2.95.

[Ru(C≡CC$_5$H$_4$NMe)(PPh$_3$)$_2$(η^5-C$_5$H$_5$)][PF$_6$] (26), [Ru(C≡CC$_6$H$_4$CH=CHC$_5$H$_4$NMe)(PPh$_3$)$_2$(η^5-C$_5$H$_5$)][PF$_6$] (27), and [Ru(C≡CC$_6$H$_4$C≡CC$_5$H$_4$NMe)(PPh$_3$)$_2$(η^5-C$_5$H$_5$)][PF$_6$] (28). Complexes **26**−**28** were prepared similarly, except that **7**, **9**, and **14**, were used, respectively. Only the preparation of **27** will be described in detail. Methyl iodide (94 μL, 1.50 mmol) was added to a solution of **9** (447 mg, 0.50 mmol) in THF (50 mL). After being stirred at room temperature in the dark for 5 h, the solution was filtered through Celite (2 cm in length) and the filtrate was pumped dry. To the resulting residue was added Tl$^+$PF$_6^-$ (192 mg, 0.55 mmol) and 50 mL of THF. The solution was then stirred for 1.5 h, and the solvent was removed under vacuum. The crude product was extracted with CH$_2$Cl$_2$ (2 × 20 mL), and the extract was filtered through Celite (2 cm in length). The volume of the solution was reduced to 8 mL, and 20 mL of hexane was added. Purple microcrystals formed after 30 min. These were collected by filtration and washed with hexane to provide analytically pure **27** in 72% yield (380 mg). Anal. Calcd for $C_{57}H_{48}F_6NP_3Ru$: C, 64.53; H, 4.56; N, 1.32. Found: C, 64.18; H, 4.32; N, 1.22.

The orange complex **26** was isolated with a yield of 76%. Anal. Calcd for $C_{49}H_{42}F_6NP_3Ru$: C, 61.38; H, 4.42; N, 1.46. Found: C, 61.01; H, 4.25; N, 1.38.

Violet complex **28** was isolated with a yield of 75%. MS (FAB): *m/e* 910 (M$^+$ − PF$_6$). Anal. Calcd for $C_{57}H_{46}F_6NP_3Ru$: C, 64.65; H, 4.38; N, 1.32. Found: C, 64.30; H, 4.25; N, 1.24.

Ru(C≡C−th)(PPh$_3$)$_2$(η^5-C$_5$H$_5$) (29; th = 5-Nitro-2-thienyl). A solution of 5-nitro-2-thienylacetylene[17] in 20 mL of MeOH was added to a solution of RuCl(PPh$_3$)$_2$(η^5-C$_5$H$_5$) (725 mg, 1.00 mmol) and NH$_4^+$PF$_6^-$ (228 mg, 1.10 mmol) in 30 mL of CH$_2$Cl$_2$. The mixture was stirred at room temperature for 20 h. The solution was then pumped dry and the residue recrystallized from CH$_2$Cl$_2$/hexane to provide a brownish powder. The brownish powder was dissolved in 15 mL of MeOH, and a MeOH solution of NaOMe (0.10 M, 15 mL) was added. The solution was stirred for 15 min, and 100 mL of H$_2$O was added. The precipitate formed was collected, washed with H$_2$O, and dried. The crude product was chromatographed using CH$_2$Cl$_2$/hexane (1:1) as eluent to afford **29** as a purple powder in 37% yield (300 mg). Anal. Calcd for $C_{47}H_{37}NO_2P_2Ru$: C, 69.62; H, 4.60; N, 1.73. Found: C, 69.39; H, 4.48; N, 1.64.

Crystallographic Studies. Crystals of **19** were grown by slow diffusion of hexane into a concentrated solution of complex **19** in CH$_2$Cl$_2$. Crystals were mounted on a glass fiber covered with epoxy. Diffraction measurements were made on an Enraf-Nonius CAD4 diffractometer by using graphite-monochromated Mo Kα radiation (λ = 0.7107 Å) with the θ−2θ scan mode. Unit cells were determined by centering 25 reflections in the suitable 2θ range. Other relevant experimental details are listed in Table 1. The structure was solved by direct methods using NRCVAX[18] and refined by full-matrix least squares (based on F^2) using SHELXL-93.[19] All non-hydrogen atoms were refined with anisotropic displacement parameters, and all hydrogen atoms were placed in idealized positions. The selected interatomic distances and bond angles are given in Table 2. All other crystal data for **19** are given in the Supporting Information.

(17) Vech, D.; Kovac, J.; Dandarova, M. *Tetrahedron Lett.* **1980**, *21*, 969.
(18) Gabe, E. J.; LePage, Y.; Charland, J. P.; Lee, F. L.; White, P. S. *J. Appl. Crystallogr.* **1989**, *22*, 384.
(19) Sheldrick, G. M. SHELXL-93, Program for Crystal Structure Refinement; University of Gottingen, Gottingen, Germany, 1993.

Table 1. Crystal Data for Compound 19

chem formula	$C_{68}H_{52}NO_4P_3FeRuW$
fw	1380.79
cryst size, mm	0.24 × 0.16 × 0.14
cryst system	triclinic
space group	$P\bar{1}$
a, Å	14.270(2)
b, Å	16.106(2)
c, Å	16.147(2)
α, deg	103.19(3)
β, deg	106.65(3)
γ, deg	108.32(3)
V, Å^3	3162(1)
Z	2
T, °C	+20
F(000)	1376
λ(Mo Kα), Å	0.7107
ρ_{calcd}, g cm^{-3}	1.450
μ, cm^{-1}	24.0
transmissn coeff	1.00−0.87
$2\theta_{max}$, deg	45
hkl range	−15 to +14, 0−17, −17 to +16
total no. of rflns	8934
no. of unique rflns	8258
no. of obsd rflns ($I > 2.0\sigma(I)$)	5764
no. of refined params	712
R^a	0.046
$R_w(F^2)^b$	0.14
GOF$(F^2)^c$	1.04

[a] $R = \sum||F_o| - |F_c||/\sum|F_o|$. [b] $w = 1/[\sigma^2(F_o^2 + (0.1025P)^2$, where $P = (\mathrm{Max}(F_o^2, 0) + 2F_c^2)/3$. [c] $\mathrm{GOF} = [\sum w(F_o^2 - F_c^2)^2/(n - p)]^{1/2}$, where n = number of observed reflections and p = number of variables.

Table 2. Selected Bond Distances (Å) and Angles (deg) for Complex 19

Distances			
Ru−C1	2.24(1)	Fe−C21	2.03(1)
Ru−C2	2.26(1)	Fe−C22	2.04(1)
Ru−C3	2.25(1)	Fe−C23	2.01(1)
Ru−C4	2.26(1)	Fe−C24	2.02(1)
Ru−C5	2.24(1)	Fe−C25	2.05(1)
Ru−C6	1.99(1)	Fe−C26	2.05(1)
Ru−P2	2.297(3)	C6−C7	1.21(1)
Ru−P3	2.284(3)	C7−C8	1.42(2)
W−C13	1.96(1)	C8−C9	1.43(2)
W−C14	1.98(1)	C9−C10	1.37(2)
W−C15	2.03(1)	C10−N	1.34(1)
W−C16	2.02(1)	N−C11	1.35(1)
W−N	2.263(8)	C11−C12	1.39(2)
W−P1	2.548(3)	C8−C12	1.40(2)
Fe−C17	2.02(1)	C13−O13	1.17(1)
Fe−C18	2.02(1)	C14−O14	1.14(1)
Fe−C19	2.03(1)	C15−O15	1.14(2)
Fe−C20	2.05(1)	C16−O16	1.13(2)
Angles			
N−W−C13	175.7(4)	C15−W−C16	173.8(5)
N−W−C14	90.6(4)	C15−W−P1	98.0(4)
N−W−C15	89.4(4)	C16−W−P1	86.3(4)
N−W−C16	95.1(4)	P2−Ru−P3	97.7(1)
N−W−P1	88.1(2)	C6−Ru−P2	85.8(3)
C13−W−C14	89.0(4)	C6−Ru−P3	89.8(3)
C13−W−C15	86.2(5)	Ru−C6−C7	175.9(9)
C13−W−C16	89.2(5)	C6−C7−C8	180(1)
C13−W−P1	92.8(3)	C7−C8−C9	122(1)
C14−W−C15	88.9(6)	C7−C8−C12	123.0(9)
C14−W−C16	86.8(6)	W−N−C10	123.0(6)
C14−W−P1	172.9(5)	W−N−C11	121.9(7)

Results and Discussion

Synthesis and Characterization of Ruthenium Complexes with a Pendant Pyridine. Two new conjugated terminal alkynes with a pendant pyridine, **5** and **12**, can be synthesized in good yield via Sonogashira coupling[20] or Heck type coupling[21] catalyzed by $PdCl_2(PPh_3)_2$ or $Pd(OAc)_2$, as depicted in Scheme 1. Metal vinylidene complexes are ubiquitous in the reactions of terminal alkynes with coordinatively unsaturated metal complexes.[22] Due to the intrinsic basicity of the pyridine, reactions of 4-ethynylpyridine, **5**, and **12** with $Ru(\eta^5\text{-}C_5H_5)(PPh_3)_2Cl$ appear to be somewhat different from those of regular terminal alkynes (Scheme 2). From the reaction of 4-ethynylpyridine, ruthenium σ-acetylide species with a pendant pyridinium, $[Ru(C{\equiv}CC_5H_4NH)L_2(\eta^5\text{-}C_5H_5)]^+$ ($\mathbf{1}^+$, L = PPh_3; $\mathbf{2}^+$, L = $^1/_2$ dppf), were obtained instead of $[Ru({=}C{=}C(H)C_5H_4N)L_2(\eta^5\text{-}C_5H_5)]^+$. If **5** is used instead of 4-ethynylpyridine, the product is isolated as a mixture of $[Ru(C{\equiv}CC_6H_4CH{=}C(H)C_5H_4NH)(PPh_3)_2(\eta^5\text{-}C_5H_5)]^+$ ($\mathbf{6a}^+$) and $[Ru({=}C{=}C(H)C_6H_4CH{=}C(H)C_5H_4N)(PPh_3)_2(\eta^5\text{-}C_5H_5)]^+$ ($\mathbf{6b}^+$). A similar reaction of **12** provides a mixture of $Ru({=}C{=}C(H)C_6H_4C{\equiv}CC_5H_4N)(PPh_3)_2(\eta^5\text{-}C_5H_5)^+$ ($\mathbf{13b}^+$) and $Ru(C{\equiv}CC_6H_4C{\equiv}CC_5H_4NH)(PPh_3)_2(\eta^5\text{-}C_5H_5)^+$ ($\mathbf{13a}^+$). In these reactions, it is likely that a vinylidene complex formed as the primary product, which is then converted to a pyridinium species. The variable-temperature ^1H and $^{31}P\{^1H\}$ NMR spectra (Figures 1 and 2) confirm the presence of a rapid exchange between the two isomers of $\mathbf{6}^+$, the pyridinium (**6a**) and the vinylidene (**6b**) species. The limiting spectra were reached when the temperature was lowered to 243 K, at which point $\mathbf{6a}^+$ and $\mathbf{6b}^+$ exist in a ratio of 8.5/10. For $\mathbf{13}^+$, the vinylidene (isomer **b**) and the pyridinium (isomer **a**) species are also in equilibrium, and the ratio of $\mathbf{13a}^+$ and $\mathbf{13b}^+$ is 1/6. The relative proportion of the vinylidene isomer vs the pyridinium isomer has to be related to the acidity of the β-H, and the basicity of the pendant pyridine, in the corresponding vinylidene intermediates. The phosphine ligands at ruthenium likely act only as spectators in these reactions, at least in case of the reactions of 4-ethynylpyridine.

Formation of a vinylidene complex can be induced if the nitrogen atom of 4-ethynylpyridine and **5** is protonated, methylated, or ligated to a metal fragment (Scheme 3). Although it proved difficult to isolate analytically pure dicationic vinylidene species **30**−**33**, these species were fully characterized by spectroscopic data.[23] All of these and the aforementioned vinylidenes exhibit characteristic chemical shifts and a small cou-

(20) Sonogashira, K. In *Comprehensive Organic Synthesis*; Trost, B. M., Fleming, I., Eds.; Pergamon: Oxford, U.K., 1991; Vol. 3, pp 521−548.

(21) (a) Cabri, W.; Candiani, I. *Acc. Chem. Res.* **1995**, *28*, 2. (b) Heck, R. F. *Palladium Reagents in Organic Syntheses*; Academic Press: New York, 1985.

(22) (a) Bruce, M. I. *Chem. Rev.* **1991**, *91*, 270. (b) Bruce, M. I.; Swincer, A. G. *Adv. Organomet. Chem.* **1983**, *22*, 59.

(23) Selected spectral data for the dicationic derivatives are listed below. **30**: ^1H NMR (acetone-d_6) δ 8.50 (d, 2 H, J = 6.6 Hz, NCH), 7.60 (d, 2 H, NCHCH), 7.55−7.18 (m, 30 H, Ph), 6.30 (t, J_{H-P} = 1.8, Ru=C=CH), 5.80 (s, 5 H, C_5H_5); $^{13}C\{^1H\}$ NMR (acetone-d_6) δ 348.01 (t, J_{C-P} = 14.2 Hz, Ru=C), 157.78 (s, NCHCHC), 141.25 (s, NCH), 134.35 (t, J_{C-P} = 5.1, PCCH), 134.06 (m, PC), 132.32 (s, PCCHCHC), 129.87 (t, J_{C-P} = 4.2, PCCHCH), 123.03 (s, NCHCH), 117.92 (s, Ru=C=C), 97.55 (s, C_5H_5); $^{31}P\{^1H\}$ NMR (acetone-d_6) δ 37.3 (s, RuP); λ_{max} 372 nm^{-1} (CH_2Cl_2). **31**: ^1H NMR (acetone-d_6) δ 8.89 (d, 2 H, J = 6.7 Hz, NCH), 8.30 (d, 2 H, NCHCH), 8.01 (d, 1 H, J = 16.4, CH=), 7.70 (d, 2 H, J = 5.3, C_6H_4), 7.51−7.17 (m, 33 H, PPh_3 and C_6H_4 and CH=), 5.80 (t, J_{H-P} = 2.4, Ru=C=CH), 5.62 (s, 5 H, C_5H_5); $^{31}P\{^1H\}$ NMR (acetone-d_6) δ 40.9 (s, RuP); λ_{max} 420 nm^{-1} (CH_2Cl_2). **32**: ^1H NMR (acetone-d_6) δ 8.47 (d, 2 H, J = 6.5 Hz, NCH), 7.54−7.17 (m, 30 H, Ph and NCHCH), 6.24 (t, J_{H-P} = 2.0, Ru=C=CH), 5.79 (s, 5 H, C_5H_5), 4.32 (s, 3 H, NCH_3); $^{31}P\{^1H\}$ NMR (acetone-d_6) δ 37.7 (s, RuP); λ_{max} 375 nm^{-1} (CH_2Cl_2). **33**: ^1H NMR (acetone-d_6) δ 8.85 (d, 2 H, J = 6.8 Hz, NCH), 8.23 (d, 2 H, NCHCH), 7.96 (d, 1 H, J = 16.3, CH=CH), 7.66 (2 H, J = 8.3, C_6H_4), 7.51−7.16 (m, 30 H, Ph), 7.45 (d, 1 H, J = 16.3, CH=CH), 7.29 (2 H, J = 8.3, C_6H_4), 5.79 (t, J_{H-P} = 2.4, Ru=C=CH), 5.63 (s, 5 H, C_5H_5), 4.48 (s, 3 H, NCH_3); $^{13}C\{^1H\}$ NMR (acetone-d_6) δ 355.69 (t, J_{C-P} = 14.7, Ru=C), 154.44 (s, NCHCHC), 145.91 (s, NCH), 141.59 (s, C_6H_4CH=CH), 134.47 (m, PC), 134.40, 129.74, 128.46, 120.19 (s, C_6H_4CH=CH), 134.28 (t, J_{C-P} = 4.5, PCCH), 131.97 (s, PCCHCHC), 129.62 (t, J_{C-P} = 4.5, PCCHCH), 128.41 (s, C_6H_4CH=CH), 124.66 (s, NCHCH), 123.13 (s, Ru=C=C), 96.49 (s, C_5H_5), 47.97 (s, NCH$_3$); $^{31}P\{^1H\}$ NMR (acetone-d_6) δ 40.9 (s, RuP); λ_{max} 434 nm^{-1} (CH_2Cl_2).

Scheme 1

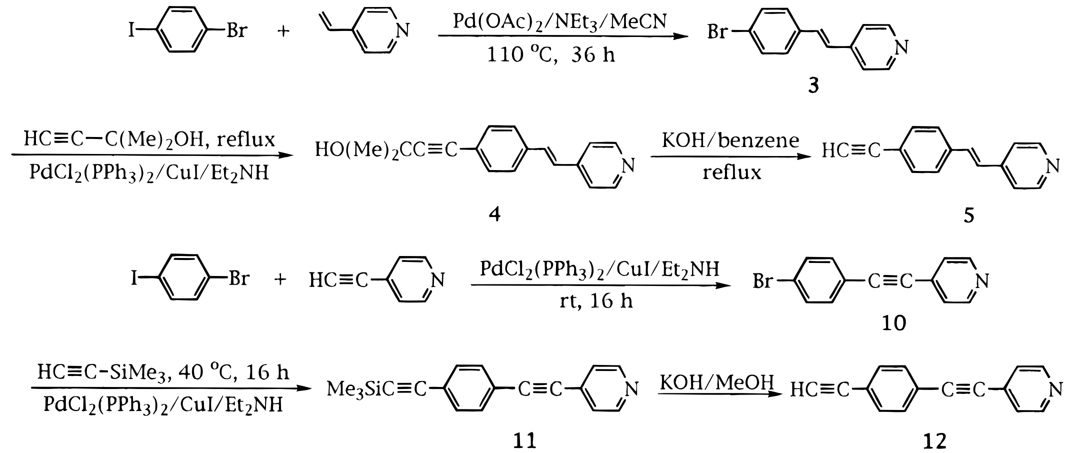

Scheme 2

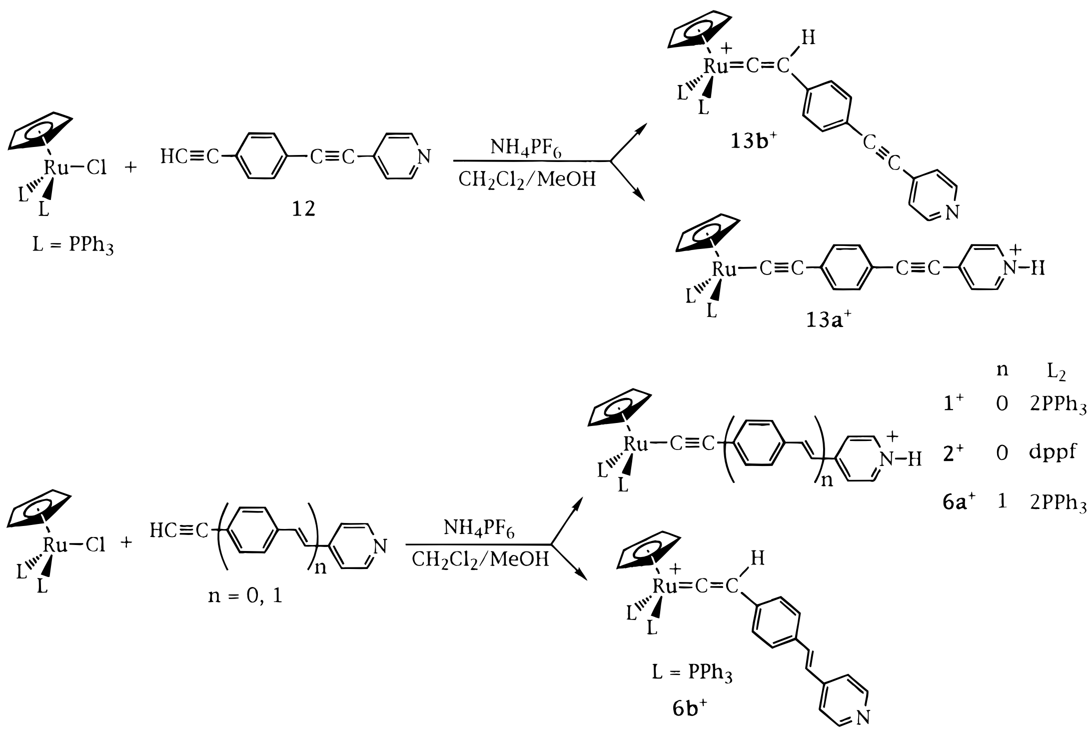

pling to two equivalent phosphorus atoms (**6b**, δ 5.75, J = 2.4 Hz; **13b**, δ 5.82, J = 2.5 Hz; **30**, δ 6.30, J = 1.8 Hz; **31**, δ 5.80, J = 2.4 Hz; **32**, δ 6.24, J = 2.0 Hz; **33**, δ 5.79, J = 2.4 Hz; **24**, δ 5.90, J = 2.1 Hz) for β-H. The chemical shifts of α- and β-carbons of these complexes in the $^{13}C\{^1H\}$ NMR spectra (**30**, C_α δ 348.01, J_{C-P} = 14.2 Hz, C_β δ 117.92; **33**, C_α δ 355.69, J_{C-P} = 14.7 Hz, C_β δ 123.13; **24**, C_α δ 350.08, J_{C-P} 14.1 Hz, C_β δ 117.49) are also consistent with literature values.[22]

Removal of the β-H atoms of the vinylidene complexes, or the protons bonded to the pyridine, by methoxide or DBU causes the formation of ruthenium σ-acetylide complexes which contain a pendant pyridine. As expected,[24] the pyridine is capable of ligation to a metal fragment and useful for construction of several dinuclear metal complexes, $Ru(C{\equiv}CC_5H_4N\{W(CO)_4L'\})(L)_2(\eta^5\text{-}C_5H_5)$ (**15**, $n = 0$, L = PPh_3, L′ = CO; **16**, $n = 0$, L = PPh_3, L′ = PPh_3; **17**, $n = 0$, L = PPh_3, L′ = PMe_3; **18**, $n = 0$, L = $^1/_2$ dppf, L′ = CO; **19**, $n = 0$, L = $^1/_2$ dppf, L′ = PPh_3; **20**, $n = 0$, L = $^1/_2$ dppf, L′ = PMe_3) and $Ru(C{\equiv}C(C_6H_4CH{=}CH)_nC_5H_4N\{W(CO)_3(dppe)\})(PPh_3)_2(\eta^5\text{-}C_5H_5)$ (**21**, $n = 0$; **22**, $n = 1$). An X-ray structural analysis for complex **19** was carried out (vide infra). Conversion of the pendant pyridine to pyridinium may also be achieved by treating the complexes with methyl iodide (Scheme 4).

The spectroscopic properties (Table 3) of the new complexes in this study are consistent with their formulations. The three moderate/strong carbonyl stretching bands for **15** and **18** in the infrared spectra are characteristic of a C_{4v} arrangement of the carbonyl ligands at the tungsten center, and the three moderate/strong carbonyl stretching bands for **16**, **17**, **19**, and **20** require that the phosphorus donor ligand and pyridine be mutually cis at the tungsten center. The three carbonyl stretching bands and the magnetic equivalency of the phosphorus nuclei in dppe suggest that the three carbonyl ligands in **21** and **22** are in a facial disposition. A symmetrical bpy ligand and two intense carbonyl stretching bands in **23**−**25** also imply a facial disposition of the three carbonyl ligands at the rhenium center. In

(24) (a) Balzani, V.; Juris, A.; Venturi, M.; Campagna, S.; Serroni, S. *Chem. Rev.* **1996**, *96*, 759. (b) Geoffroy, G. L., Wrighton, M. S., Eds. *Organometallic Photochemistry*; Academia: New York, 1979.

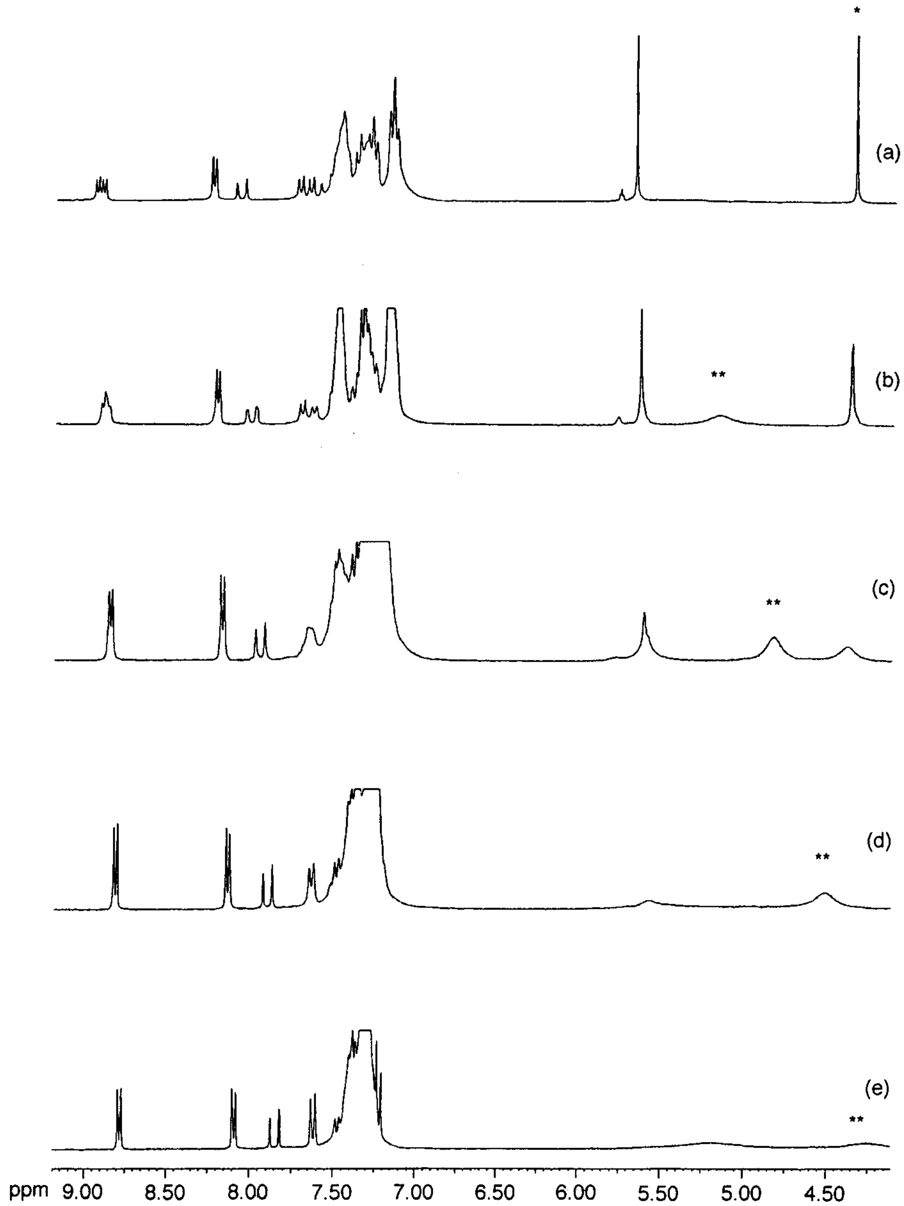

Figure 1. Variable-temperature ^{1}H NMR spectra of complex **6** in acetone-d_6 at (a) 243, (b) 263, (c) 283, (d) 303, and (e) 333 K. Peaks marked with an asterisk are from Cp of **6a**, and those marked with two asterisks are from H_2O.

general, the carbonyl stretching frequencies decrease as the π-accepting ability of phosphine ligands decreases or the number of phosphine ligands increases. In ^{31}P NMR spectra, the signal for the phosphine ligand coordinated to the tungsten atom is accompanied by a pair of satellites with $^1J_{P-W} = 228-240$ Hz, in agreement with literature values.[25] The ^{13}C{^{1}H} NMR spectra for vinylidene complexes have been discussed earlier. The ^{13}C{^{1}H} NMR spectra for two of the σ-acetylide complexes, **7** and **9**, were also checked and found to be normal (**7**, C_α t, δ 132.82, $J_{C-P} = 24.3$ Hz, C_β δ 113.65; **9**, C_α t, δ 123.37, $J_{C-P} = 24.7$ Hz, C_β δ 115.56).[22] Another unique feature of the σ-acetylide complexes is the existence of a ν(C≡C) stretching (2025−2070 cm^{-1}) in the infrared spectra.

Optical Absorption Spectra. Table 4 illustrates the optical absorption spectra of new organometallic complexes in CH_2Cl_2 and/or CH_3CN. Ligation of the pendant pyridine in **7**−**9** to metal carbonyl fragments results in a bathochromic shift of λ_{max}: for instance, **7** (338 nm, in CH_2Cl_2) vs **15** (397 nm), **16** (400 nm), **17** (380 nm), **21** (357 nm), and **25** (402 nm), **8** (339 nm) vs **18** (396 nm), **19** (403 nm), and **20** (380 nm) and **9** (419 nm) vs **22** (462 nm). This observation is consistent with the presence of a charge-transfer band from the electron-donor ruthenium fragment to the electron-acceptor metal carbonyl fragment.[10] There is considerable superposition of this band with the metal-to-pyridine π^* charge-transfer band of the tungsten carbonyl fragment, however. In contrast, this charge-transfer band in **25** is free from the rhenium-to-pyridine π^* charge-transfer band, judging from comparison of the spectra between **23** and **25**. The pyridinium moiety, being a good electron acceptor,[26] has been reported to induce a strong low-lying charge-transfer band upon connecting to an organometallic electron donor.[27] The bathochromic shift of λ_{max} is even greater if the pendant pyridine is converted to pyridinium: for example, **7** (338 nm, in CH_2Cl_2) vs **1** (446 nm) and **26** (460 nm), **8** (339 nm) vs

(25) Pregosin, P. S.; Kunz, R. W. *^{31}P and ^{13}C NMR of Transition Metal Phosphine Complexes*; Springer-Verlag: New York, 1979.

(26) (a) Marder, S. R.; Perry, J. W.; Yakymyshyn, C. P. *Chem. Mater.* **1994**, *6*, 1137. (b) Marder, S. R.; Perry, J. W.; Tiemann, B. G.; Schaefer, W. P. *Organometallics* **1991**, *10*, 1896.

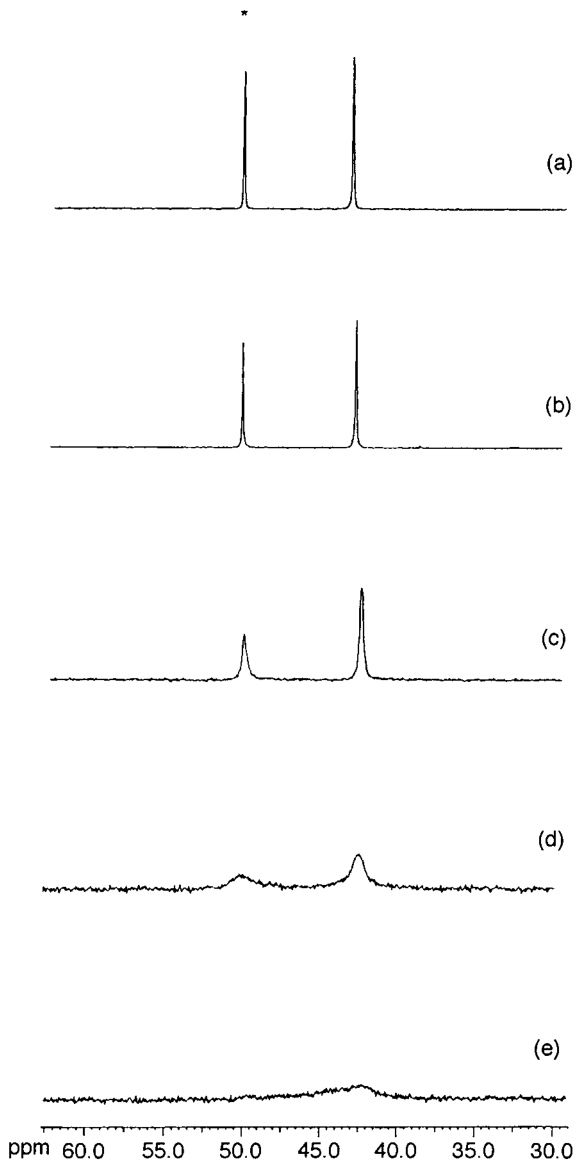

Figure 2. Variable-temperature $^{31}P\{^{1}H\}$ NMR spectra of complex **6** in acetone-d_6 at (a) 243, (b) 263, (c) 283, (d) 303, and (e) 333 K. Peaks marked with an asterisk are from **6a**.

2 (441 nm), **9** (419 nm) vs **27** (582 nm), and **14** (397 nm) vs **28** (558 nm). This effect seems to be much larger than that of analogous ruthenium σ-acetylide complexes in which the nitrophenyl moiety is an electron acceptor.[8b] It is well-known that elongation of the conjugation length in a second-order nonlinear optical organic chromophore results in a decrease in the energy of the charge-transfer band.[28] In our case, elongation of the conjugation also causes a dramatic red shift of the charge-transfer band, i.e., **26** (460 nm) vs **27** (582 nm) and **28** (558 nm). The diminished red shift in **28** compared to that in **27** may be attributed to the mismatch of a phenyl p orbital and an alkynyl p orbital in energy.[28b,29] Complexes with an end-capping pyridinium (**1**, **2**, **26**−**28**) exhibit a hypsochromic shift of λ_{max} upon changing from CH_2Cl_2 to CH_3CN. The negative solvatochromic behavior is larger for complexes with extension of the conjugation length (**26** vs **27** and **28**). Organometallic sesquifulvalene complexes with a cationic electron acceptor were also reported to have a similar hypsochromic shift of λ_{max} upon changing from CH_2Cl_2 to a polar solvent (CH_3CN or acetone).[30] The neutral complex Ru(C≡$CC_6H_4NO_2$-4)$(PPh_3)_2(\eta^5$-$C_5H_5)$ was reported to have a bathochromic shift of λ_{max} as the solvent polarity increases (437 nm in cyclohexane; 476 nm in dimethylformamide). We observe a similar trend for the neutral complex **29** (λ_{max} 506 nm in benzene and 535 nm in dimethylformamide). It is interesting to note that the charge-transfer band of complex **29** is significantly longer than that of Ru(C≡$CC_6H_4NO_2$-4)$(PPh_3)_2$-$(\eta^5$-$C_5H_5)$, which is in accordance with the fact that a nitrothienyl moiety is a better electron acceptor than a nitrophenyl moiety.[31]

Previously we mentioned that the dicationic vinylidene complexes **30** and **31** could be synthesized by the method described in Scheme 3. They may also be prepared by double protonation of **7** and **9** with a strong acid, HBF_4 or CF_3CO_2H. The λ_{max} values of **30** (372 nm in CH_2Cl_2) and **31** (410 nm in CH_2Cl_2) are smaller than those of **1** and **6a**, suggesting a lesser degree of electron delocalization in **30** and **31** than in **1** and **6a**. Use of optical absorption spectra in monitoring protonation/deprotonation in some of the complexes proved to be informative. For instance, gradual addition of NEt_3 to a CH_2Cl_2 solution of **30** first results in removal of a β-H and formation of **1**, which is then transformed to **4** (Figure 3). This result illustrates that the pyridyl nitrogen is more basic than the β-carbon in **7** and provides a rationale for the absence of a vinylidene intermediate in the formation of **1** (vide supra). Monitoring the protonation of **9** indicated first the formation of **6a** and **6b**; however, both **6a** and **6b** were then converted to **31**. Conversely, the deprotonation of **31** resulted in sequential formation of **6a**/**6b** and **9**. Protonation of **14** and the deprotonation of the dication of **14** were followed similarly, both via the intermediates **13a**/**13b**, consistent with the observation from the NMR spectra.

Electrochemistry. The oxidation potentials (Table 5) for the metals Ru, Fe, W, and Re can be readily assigned. In general, the ruthenium and iron complexes have reversible oxidation waves (Ru(II)/Ru(III) and Fe(II)/Fe(III)). Similar to what has been reported for Cp_2-Fe−[C≡C−$C_6H_4]_n$−SO_2Me,[32] and bimetallic sesquifulvalene complexes,[30b] increase of the conjugation length lowers the oxidation potential of the metal (**7** vs **9** and **14** and **26** vs **27** and **28**). Humphrey reported that Ru-(C≡$CC_6H_4NO_2$-4)$(PPh_3)_2(\eta^5$-$C_5H_5)$ was oxidized at potential 0.2 V higher than Ru(C≡$CC_6H_5)(PPh_3)_2(\eta^5$-$C_5H_5)$.[8a] We also found that ruthenium is oxidized at higher potential upon increasing the acceptor strength of the acetylide (**7** vs **1** and **26**; **9** vs **27**; **14** vs **28**). The effect is decreased considerably in **27** and **28**, and this can be attributed to the longer distance between ruthe-

(27) (a) Alain, V.; Fort, A.; Marguerite, B.; Chen, C. T. *Inorg. Chim. Acta* **1996**, *242*, 43. (b) Alain, V.; Blanchard-Desce, B.; Chen, C. T.; Marder, S. R.; Fort, A.; Barzoukas, M. *Synth. Met.*, in press. (c) Lin, J. T.; Wu, J. J.; Li, C. S.; Wen, Y. S.; Lin, K. J. *Organometallics* **1996**, *15*, 5028.
(28) (a) Tiemann, B. G.; Cheng, L. T.; Marder, S. R. *J. Chem. Soc., Chem. Commun.* **1993**, 735. (b) Cheng, L. T.; Tam, W.; Marder, S. R.; Stiegman, A. E.; Rikken, G.; Spangler, C. W. *J. Phys. Chem.* **1991**, *95*, 10643.
(29) Stiegman, A. E.; Graham, E.; Perry, K. J.; Khundkar, L. R.; Cheng, L. T.; Perry, J. W. *J. Am. Chem. Soc.* **1991**, *113*, 7658.
(30) (a) Tamm, M.; Grzegorzewski, A.; Steiner, T.; Jentzsch, T.; Werncke, W. *Organometallics* **1996**, *15*, 4984. (b) Behrens, U.; Brussaard, H.; Hagenau, U.; Heck, J.; Hendrickx, E.; Kornich, J.; van der Linden, J. G. M.; Persoons, A.; Spek, A. L.; Veldman, N.; Voss, B.; Wong, H. *Chem. Eur. J.* **1996**, *2*, 98.
(31) Rao, V. P.; Cai, Y. M.; Jen, A. K. Y. *J. Chem. Soc., Chem. Commun.* **1994**, 1689.
(32) Hsung, R. P.; Chidsey, C. E. D.; Sita, L. R. *Organometallics* **1995**, *14*, 4808.

Scheme 3

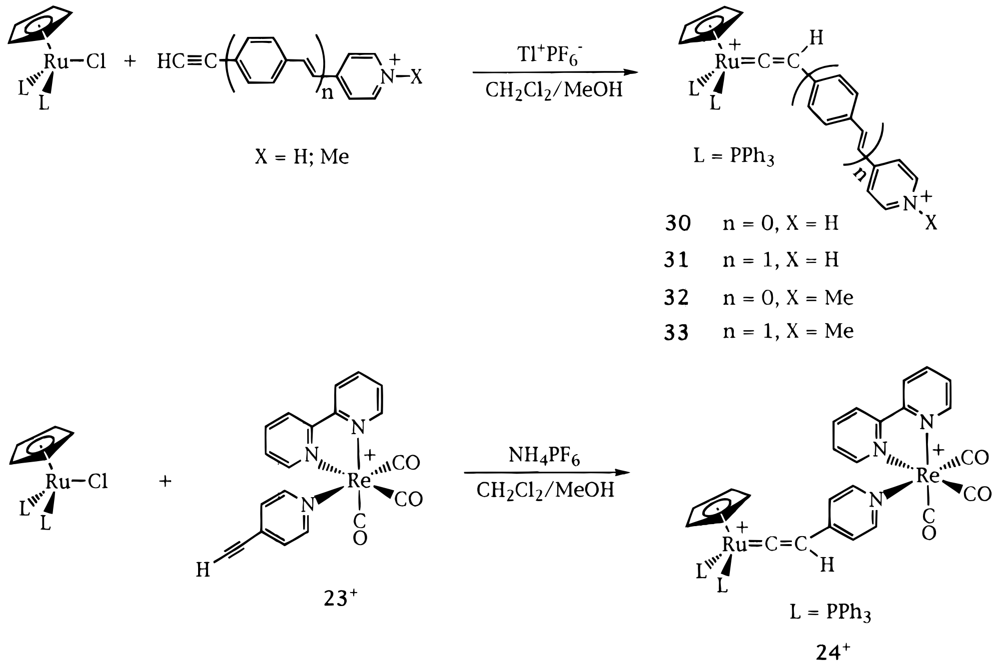

Scheme 4

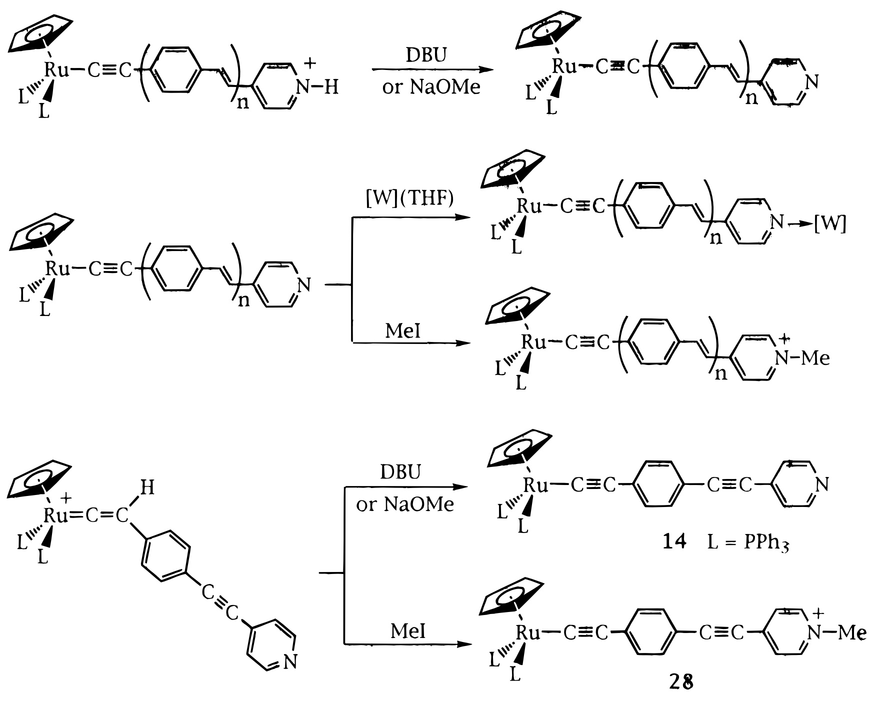

compd	n	L	[W]
15	0	PPh_3	$W(CO)_5$
16	0	PPh_3	$W(CO)_4(PPh_3)$
17	0	PPh_3	$W(CO)_4(PMe_3)$
18	0	$1/2\{(C_5H_4PPh_2)_2Fe\}$	$W(CO)_5$
19	0	$1/2\{(C_5H_4PPh_2)_2Fe\}$	$W(CO)_4(PPh_3)$
20	0	$1/2\{(C_5H_4PPh_2)_2Fe\}$	$W(CO)_4(PMe_3)$
21	0	PPh_3	$W(CO)_3(\eta^2\text{-dppe})$
22	1	PPh_3	$W(CO)_3(\eta^2\text{-dppe})$

nium and pyridinium in **27** (or **28**) than in **9** (or **14**). The oxidation of the tungsten atom is an irreversible process, and the oxidation potentials of the homologous complexes are in the order $W(CO)_5 > W(CO)_4(PPh_3) > W(CO)_4(PMe_3) > W(CO)_3(\eta^2\text{-dppe})$, which is in accordance with the π-accepting ability of the ligands.

Similar to our previous observation,[9] the reduction potential of the pendant pyridine in **7**, **8**, **9**, and **14** appears to be very negative (<−2.50 V). A reliable reduction potential for the pyridine in **15**−**22** was not observed, possibly because ligation of pyridine to metal carbonyls dowa not significantly lower the π^* orbital of pyridine, or the complexes were not stable upon reduction. A reversible reduction in complex **25** is most likely to be due to reduction of the bipyridine ligand, which generally has a lower lying π^* orbital than pyridine.

Table 3. IR Spectra in the ν(CO) Region and ^{1}H and ^{31}P{^{1}H} NMR Spectra of the Compounds

compd	ν(CO), *ν(C≡C)*,[a] cm^{-1}	δ (ppm)[b,c] (*J*(Hz))	δ (ppm)[b,d] (*J*(Hz))
1	*2014 m*	8.01 (d, 2 H, *J* = 6.9, NC*H*), 7.29−7.10 (m, 30 H, Ph), 6.90 (d, 2 H, NCHC*H*), 4.45 (s, 5 H, C_5H_5)	50.3 (s, 2 P, Ru*P*), −145 (heptet, 1 P, J_{P-F} = 702, PF_6)
2	*2012 m*	8.09 (d, 2 H, *J* = 6.9, NC*H*), 7.62−7.09 (m, 20 H, Ph), 7.08 (d, 2 H, NCHC*H*), 4.87 (br, 2 H, C_5H_4), 4.41 (s, 5 H, C_5H_5), 4.38 (br, 2 H, C_5H_4), 4.29 (br, 2 H, C_5H_4), 4.11 (br, 2 H, C_5H_4)	55.4 (s, 2 P, Ru*P*), −145 (heptet, 1 P, J_{P-F} = 702, PF_6)
5	*2091 m*	8.57 (d, 2 H, *J* = 6.1, NC*H*), 7.48 (d, 2 H, *J* = 9.1, C_6H_4), 7.47 (d, 2 H, C_6H_4), 7.34 (d, 2 H, NCHC*H*), 7.25 (d, 2 H, *J* = 16.3, =C*H*), 7.01 (d, 2 H, =C*H*), 3.14 (s, 1 H, ≡C*H*)	
6[e]	*2052 m*	**6a**: 8.94 (d, 2 H, *J* = 6.6, NC*H*), 8.24 (d, 2 H, NCHC*H*), 8.08 (d, 1 H, *J* = 16.7, C*H*=), 7.73 (d, 2 H, *J* = 7.3, C_6H_4), 7.56−7.10 (m, 33 H, Ph & C_6H_4 & =C*H*), 4.36 (s, 5 H, C_5H_5)	**6a**: 48.3 (s, 2 P, Ru*P*), −145 (heptet, 2 P, J_{P-F} = 702, PF_6)
		6b: 8.88 (d, 2 H, *J* = 6.6, NC*H*), 8.24 (d, 2 H, NCHC*H*), 8.08 (d, 1 H, *J* = 16.7, C*H*=), 7.65 (d, 2 H, *J* = 7.4, C_6H_4), 7.56−7.10 (m, 33 H, Ph & C_6H_4 & =C*H*), 5.75 (t, 1 H, J_{H-P} = 2.4, Ru=C=C*H*), 4.36 (s, 5 H, C_5H_5)	**6b**: 42.5 (s, 2 P, Ru*P*), −145 (heptet, 2 P, J_{P-F} = 702, PF_6)
7[f]	*2070 m*	8.26 (d, 2 H, *J* = 6.3, NC*H*), 7.43−7.05 (m, 30 H, Ph), 6.85 (d, 2 H, NCHC*H*), 4.32 (s, 5 H, C_5H_5)	50.8 (s)
8	*2070 m*	8.30 (d, 2 H, *J* = 6.0, NC*H*), 7.78−7.29 (m, 20 H, Ph), 6.96 (d, 2 H, NCHC*H*), 5.15 (br, 2 H, C_5H_4), 4.30 (br, 7 H, C_5H_5 & C_5H_4), 4.16 (br, 2 H, C_5H_4), 3.98 (br, 2 H, C_5H_4)	50.6 (s)
9[f]	*2065 m*	8.51 (d, 2 H, *J* = 6.2, NC*H*), 7.48−7.05 (m, 34 H, Ph & C_6H_4), 7.32 (d, 2 H, NCHC*H*), 7.23 (d, 1 H, *J* = 16.2, C*H*=), 6.87 (d, 1 H, *J* = 16.2, C*H*=), 4.32 (s, 5 H, C_5H_5)	50.9 (s)
12		8.58 (d, 2 H, *J* = 6.1, NC*H*), 7.47 (s, 4 H, C_6H_4), 7.34 (d, 2 H, NCHC*H*), 3.18 (s, 1 H, ≡C*H*)	
13[e]	*2218 w*, 1635 w ($\nu_{C=C}$)	**13a**: 8.99 (d, 2 H, *J* = 6.3, NC*H*), 8.07 (d, 2 H, *J* = 6.3, NCHC*H*), 7.58−7.15 (m, 34 H, Ph & C_6H_4), 4.37 (s, 5 H, C_5H_5)	**13a**: 50.4 (s, 2 P, Ru*P*), −143 (heptet, 2 P, J_{P-F} = 710, PF_6)
		13b: 8.87 (d, 2 H, *J* = 6.3, NC*H*), 7.87 (d, 2 H, *J* = 6.3, NCHC*H*), 7.58−7.15 (m, 34 H, Ph & C_6H_4), 5.82 (t, 1 H, J_{H-P} = 2.5, Ru=C=C*H*), 5.71 (s, 5 H, C_5H_5)	**13b**: 41.9 (s, 2 P, Ru*P*), −143 (heptet, 2 P, J_{P-F} = 710, PF_6)
14	*2212 w*, *2061 m*	8.55 (d, 2 H, *J* = 6.0, NC*H*), 7.33 (d, 2 H, NCHC*H*), 7.46−7.05 (m, 34 H, Ph & C_6H_4), 4.32 (s, 5 H, C_5H_5)	50.8 (s)
15	2026 m, 1922 vs, 1885 s, *2045 m*	8.53 (d, 2 H, *J* = 5.4, NC*H*), 7.45−7.16 (m, 30 H, Ph), 6.94 (d, 2 H, NCHC*H*), 4.43 (s, 5 H, C_5H_5)	55.6 (s)
16	2007 m, 1886 vs, 1837 s, *2043 m*	8.07 (d, 2 H, *J* = 6.3, NC*H*), 7.57−7.16 (m, 45 H, Ph), 6.54 (d, 2 H, NCHC*H*), 4.41 (s, 5 H, C_5H_5)	55.8 (s, 2 P, Ru*P*), 35.7 (s with satellites, 1 P, J_{P-W} = 232)
17	2003 m, 1875 vs, 1838 s, *2043 m*	8.36(d, 2 H, *J* = 6.0, NC*H*), 7.35−7.06 (m, 30 H, Ph), 6.60 (d, 2 H, NCHC*H*), 4.34 (s, 5 H, C_5H_5), 1.46 (d, 9 H, *J* = 7.5, Me)	55.5 (s, 2 P, Ru*P*), −21.1 (s with satellites, 1 P, J_{P-W} = 240, W*P*)
18	2067 m, 1927 vs, 1890 s, *2043 m*	8.37 (d, 2 H, *J* = 6.6, NC*H*), 7.72−7.28 (m, 20 H, Ph), 6.78 (d, 2 H, NCHC*H*), 5.28 (br, 2 H, C_5H_4), 4.39 (br, 7 H, C_5H_5 & C_5H_4), 4.23 (br, 2 H, C_5H_4), 4.03 (br, 2 H, C_5H_4)	55.5 (s)
19	2007 m, 1886 vs, 1843 s, *2044 m*	8.08 (d, 2 H, *J* = 6.9, NC*H*), 7.47−7.31 (m, 35 H, Ph), 6.65 (d, 2 H, NCHC*H*), 5.15 (br, 2 H, C_5H_4), 4.43 (br, 2 H, C_5H_4), 4.37 (br, 7 H, C_5H_5 & C_5H_4), 4.16 (br, 2 H, C_5H_4)	60.6 (s, 2 P, Ru*P*), 36.1 (s with satellites, 1 P, J_{P-W} = 228, W*P*)
20	2002 m, 1873 vs, 1836 s, *2042 m*	8.42 (d, 2 H, *J* = 6.3, NC*H*), 7.76−7.29 (m, 20 H, Ph), 6.72 (d, 2 H, NCHC*H*), 5.00 (br, 2 H, C_5H_4), 4.32 (br, 7 H, C_5H_5 & C_5H_4), 4.21 (br, 2 H, C_5H_4), 4.02 (br, 2 H, C_5H_4), 1.46 (d, 9 H, *J* = 7.2, Me)	55.4 (s, 2 P, Ru*P*), −25.9 (s with satellites, 1 P, J_{P-W} = 236, W*P*)
21	1914 vs, 1812 vs, 1802 sh, *2038 m*	7.69−6.85 (m, 50 H, Ph), 7.59 (d, 2 H, *J* = 6.6, NC*H*), 5.95 (d, 2 H, NCHC*H*), 4.28 (s, 5 H, C_5H_5), 2.66 (m, 4 H, CH_2)	51.1 (s, 2 P, Ru*P*), 48.1 (s with satellites, 2 P, J_{P-W} = 230, W*P*)
22	1917 m, 1820 vs, 1802 vs, *2062 m*	7.83 (d, 2 H, *J* = 6.6, NC*H*), 7.42−7.02 (m, 54 H, Ph& C_6H_4), 6.97 (d, 1 H, *J* = 16.2, C*H*=), 6.52 (d, 1 H, *J* = 16.2, C*H*=), 6.36 (d, 2 H, NCHC*H*), 4.31 (s, 5 H, C_5H_5), 2.70 (m, 4 H, CH_2)	50.9 (s, 2 P, Ru*P*), 48.9 (s with satellites, 2 P, J_{P-W} = 231, W*P*)
23	2037 vs, 1929 vs	9.45 (d, 2 H, J_{H-H} = 6.2, bpy-6,6′), 8.71 (d, 2 H, J_{H-H} = 8.2, bpy-3,3′), 8.56 (d, 2 H, *J* = 6.8, NC*H*), 8.46 (td, 2 H, J_{H-H} = 7.9; 1.5, bpy-4,4′), 7.99 (td, 2 H, J_{H-H} = 7.1; 1.2, bpy-5,5′), 7.47 (d, 2 H, NCHC*H*), 4.33 (s, 1 H, ≡C*H*)	−145 (heptet, 2 P, J_{P-F} = 702, PF_6)
24[f]	2034 vs, 1924 vs	9.38 (d, 2 H, J_{H-H} = 6.0, bpy-6,6′), 8.74 (d, 2 H, J_{H-H} = 8.1, bpy-3,3′), 8.46 (td, 2 H, J_{H-H} = 8.1; 1.5, bpy-4,4′), 8.05 (d, 2 H, J_{H-H} = 5.7, NC*H*), 7.98 (td, 2 H, J_{H-H} = 6.0; 1.2, bpy-5,5′), 7.51−6.97 (m, 30 H, Ph), 6.95 (d, 2 H, J_{H-H} = 5.7, NCHC*H*), 5.90 (t, 1 H, J_{H-P} = 2.1, Ru=C=C*H*), 5.63 (s, 5 H, C_5H_5)	38.4 (s, 2 P, Ru*P*), −145 (heptet, 2 P, J_{P-F} = 702, PF_6)
25	2031 vs, 1925 vs	9.44 (d, 2 H, J_{H-H} = 6.0, bpy-6,6′), 8.74 (d, 2 H, J_{H-H} = 8.0, bpy-3,3′), 8.47 (t, 2 H, *J* = 7.9, bpy-4,4′), 8.00 (m, 4 H, bpy-5,5′ & NC*H*), 7.33−7.10 (m, 30 H, Ph), 6.77 (d, 2 H, *J* = 6.3, NCHC*H*), 4.39 (s, 5 H, C_5H_5)	48.8 (s, 2 P, Ru*P*), −145 (heptet, 2 P, J_{P-F} = 702, PF_6)
26	*2025 m*	8.46(d, 2 H, *J* = 6.6, NC*H*), 7.40−7.20 (m, 32 H, Ph & NCHC*H*), 4.56 (s, 5 H, C_5H_5), 4.22 (s, 3 H, Me)	55.4 (s)
27	*2038 m*	8.48 (d, 2 H, *J* = 6.6, NC*H*), 7.91 (d, 2 H, NCHC*H*), 7.64 (d, 1 H, *J* = 16.1, C*H*=), 7.45−7.07 (m, 34 H, Ph & C_6H_4), 6.97 (d, 1 H, *J* = 16.1, C*H*=), 4.34 (s, 5 H, C_5H_5), 4.05 (s, 3 H, Me)	51.0 (s)
28	*2210 w*, *2055 m*	8.98 (d, 2 H, *J* = 6.8, NC*H*), 7.81 (d, 2 H, NCHC*H*), 7.44−7.04 (m, 34 H, Ph & C_6H_4), 4.52 (s, 3 H, Me), 4.33 (s, 5 H, C_5H_5)	50.8 (s)
29		7.81 (d, 1 H, *J* = 4.2, Th), 7.44−7.18 (m, 30 H, Ph), 6.50 (d, 1 H, Th), 4.46 (s, 5 H, C_5H_5)	50.4 (s)

[a] Measured in CH_2Cl_2 solution. [b] Measured in $CDCl_3$ except for **6**, **24**, and **25**, which were measured in acetone-d_6. [c] Reported in ppm relative to δ(Me_4Si) at 0 ppm. [d] Reported in ppm relative to δ(85% H_3PO_4) at 0 ppm. [e] Measured in acetone-d_6 at 243 K. [f] ^{13}C{^{1}H} NMR spectra ($CDCl_3$, in ppm relative to δ(Me_4Si) 0 ppm): **7**, 148.73 (s, N*C*), 138.46 (m, C_{ipso} of PPh_3), 137.61 (s, NCHCH*C*), 133.67 (t, J_{C-P} = 4.8, C_{ortho} of PPh_3), 132.82 (t, J_{C-P} = 24.3, Ru−*C*≡C), 128.57 (s, C_{para} of PPh_3), 127.28 (t, J_{C-P} = 3.7, C_{meta} of PPh_3), 125.16 (s, NCH*C*H), 113.65 (s, Ru−C≡*C*), 85.41 (s, C_5H_5); **9**, 149.96 (s, N*C*H), 145.28 (s, NCHCH*C*), 138.74 (m, C_{ipso} of PPh_3), 133.70 (t, J_{C-P} = 4.5, C_{ortho} of PPh_3), 133.59 (s, C_6H_4CH*C*H), 131.36 (s, *C*CH=CH), 130.81 (s, *C*HCCH=CH), 130.57 (s, C≡C*C*), 128.44 (s, C_{para} of PPh_3), 127.20 (t, J_{C-P} = 4.1, C_{meta} of PPh_3), 126.66 (s, C≡CC*C*H), 123.37 (t, J_{C-P} = 24.7, Ru−*C*≡C), 123.18 (s, C_6H_4*C*H), 120.57 (s, NCH*C*H), 115.56 (s, Ru−C≡*C*), 85.28 (s, C_5H_5); **24** (acetone-d_6), 350.08 (t, J_{C-P} = 14.1, Ru=*C*), 196.51 (s, CO), 192.51 (s, CO), 156.65 (s, bpy-2,2′), 154.84 (s, N*C*H), 151.97 (s, bpy-3,3′), 144.12 (s, NCHCH*C*), 142.37 (s, bpy-5,5′), 134.32 (t, J_{C-P} = 4.1, PC*C*H), 133.73 (m, P*C*), 132.19 (s, PCCHCH*C*), 130.03 (s, NCH*C*H), 129.72 (t, J_{C-P} = 4.6, PCCH*C*H), 125.68 (s, bpy-4,4′), 123.90 (s, bpy-6,6′), 117.49 (s, Ru=C=*C*), 97.03 (s, C_5H_5). Abbreviations: s = singlet, d = doublet, t = triplet, m = multiplet.

Table 4. Optical Absorption Spectra of Compounds (λ_{max}, nm)

compd	CH_2Cl_2	CH_3CN
1	446	432
2	441	433
6a		516[a]
6b		348[a]
7	338	336
8	339	337
9	419	410
13a		490[a]
13b		320[a]
14	397	
15	397	394
16	400	397
17	407	401
18	396	394
19	402	400
20		401
21	404	
22	462	441
23		350
25	402	398
26	460	437
27	582	520
28	558	498
29	543	526
30	372	
33	434	

[a] The measurements were taken in acetone.

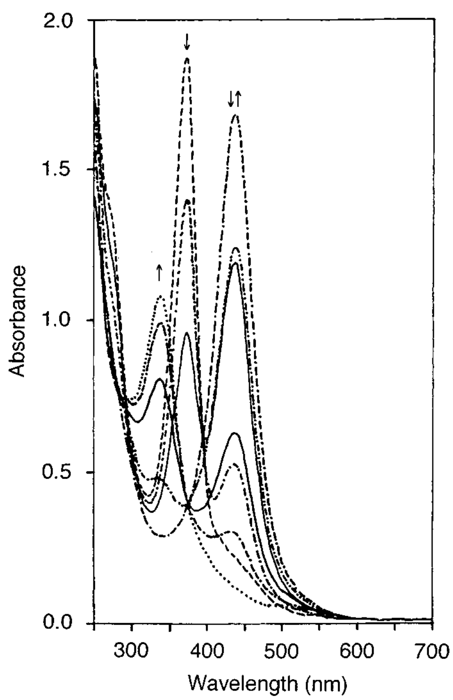

Figure 3. UV−vis spectra (in CH_2Cl_2) for the deprotonation of **29** with NEt_3: λ_{max} 372 nm (**29**), 446 nm (**1**), 338 nm (**9**). ↓ indicates the intensity is decreasing with time, ↑ indicates the intensity is increasing with time, and ↓↑ indicates the intensity is first increasing and then decreasing with time. The isosbestic points appear at 390 and 373 nm.

Complex **29** also has a reversible reduction wave, and this can be assigned to the reduction of the nitro substituent on the thienyl ring, similar to the case of $Ru(C{\equiv}CC_6H_4NO_2\text{-}4)(PPh_3)_2(\eta^5\text{-}C_5H_5)$.[8a] The irreducible reduction waves appearing at −2.00, −1.49, and −1.46 V, respectively, for complexes with a pendant 1-methyl-4-pyridiniumyl moiety (**26**−**28**) were assigned as the reduction of the pyridinium.

Theoretical studies by Kostic and Fenske[33] on $Fe(C{\equiv}CH)(PH_3)_2(\eta^5\text{-}C_5H_5)$ suggested that the LUMO is

Table 5. Redox Potentials for Complexes in CH_2Cl_2 at 298 K[a]

complex	E_{ox} (ΔEp)			
	Ru(+2/+3)	Fe(+2/+3)	W(0/+1)	E_{red} (ΔE_p)[c]
1	+0.37 (73)			
2	+0.25 (61)			
7	+0.15 (95)			>−2.50
8	+0.10 (106)	+0.48 (104)		>−2.50
9	+0.00 (84)			>−2.50
14	+0.04 (87)			>−2.50
15	+0.24 (110)		+0.62	
16	+0.22		+0.14	
17	+0.16		+0.08	
18	+0.20 (99)	+0.55	+0.55	
19	+0.26 (90)	+0.52 (99)	+0.14	
20	+0.25 (83)	+0.51 (80)	+0.06	
21	+0.17		−0.16	
22	+0.05		−0.09	
25	+0.26 (100)		+0.70[d]	−1.61 (78)
26	+0.36 (95)			−2.00 (i)
27	+0.06 (84)			−1.33 (i)
28	+0.09 (100)			−1.41 (i)
29	+0.22 (96)			−1.62(98)

[a] Analyses performed in 10^{-3} M deoxygenated CH_2Cl_2 solutions containing 0.1 M TBAP; scan rate 60 mV. All potentials in volts vs ferrocene (0.00 V with peak separation of 105 mV in CH_2Cl_2); scan range +0.8 to −1.8 V; i = irreversible process. [b] The measurements were taken in CH_2Cl_2/CH_3CN since the oxidation peak for tungsten is almost merged in the reversible peak of Fe(2+/3+) when the measurements were taken in CH_2Cl_2. [c] $\Delta E_p = E_{pa} - E_{pc}$ (mV). [d] E_{ox} (ΔE_p) for Re(+/2+).

metal-centered for σ-acetylide complexes of that type. The potential difference (E_p) between the oxidation potential of Ru and the reduction potential of the acceptor for complexes **26**−**29** seems to be in agreement with this. The E_p values are in the order **26** (2.36 V) > **29** (1.88 V) > **28** (1.50 V) > **27** (1.39 V), in accordance with the the energy of the charge-transfer band in electronic spectra (vide supra). As expected, the E_p value for complex **7** is calculated to be higher than 2.65 V because of the high-lying π* orbital of the pyridine.

NLO Measurements. Hyper Rayleigh scattering (HRS) experiments were performed on complexes **26**−**28** at a wavelength of 1064 nm with a Q-switch Nd:YAG laser (Continuum Surelite I). Solutions of *p*-nitroaniline in CH_2Cl_2 were used as external references ($\beta = 16.9 \times 10^{-30}$ esu at 1064 nm).[34] The experimental setup was described elsewhere.[35] From the HRS experiment, the first hyperpolarizabilities (β, 10^{-30} esu) of complexes **26**−**28** are determined to be 152, 1682, and 1505, respectively. Recently, it has been reported that the HRS signal is found mixed with the two-photon absorption (TPA) fluorescence at the second harmonic wavelength (532 nm).[34,36] To obtain the intrinsic β value, the TPA-induced fluorescence must be discriminated against. The TPA-induced fluorescence spectra of complexes **26**−**28** were measured (see Figure S1 in the Supporting Information) in an manner identical with that for the HRS experiment, except the interference filter was replaced by a monochromator. As shown in Figure S1, the overall spectra can be divided into two contributions: a sharp URS peak at 532 nm and a much

(33) Kostic, N. M.; Fenske, R. F. *Organometallics* **1982**, *1*, 974.
(34) Stahelin, M.; Burland, D. M.; Rice, J. E. *Chem. Phys. Lett.* **1992**, *191*, 245.
(35) Hsu, C. C.; Huang, T. H.; Zang, Y. L.; Lin, J. L.; Chen, Y. Y.; Lin, J. T.; Wu, H. H.; Wang, C. H.; Kuo, C. T.; Chen, C. H. *J. Appl. Phys.* **1996**, *80*, 5996.
(36) Flipse, M. C.; de Jonge, R.; Woudenberg, R. H.; Marsman, A. W.; van Walree, C. A.; Jenneskens, L. W. *Chem. Phys. Lett.* **1995**, *245*, 297.

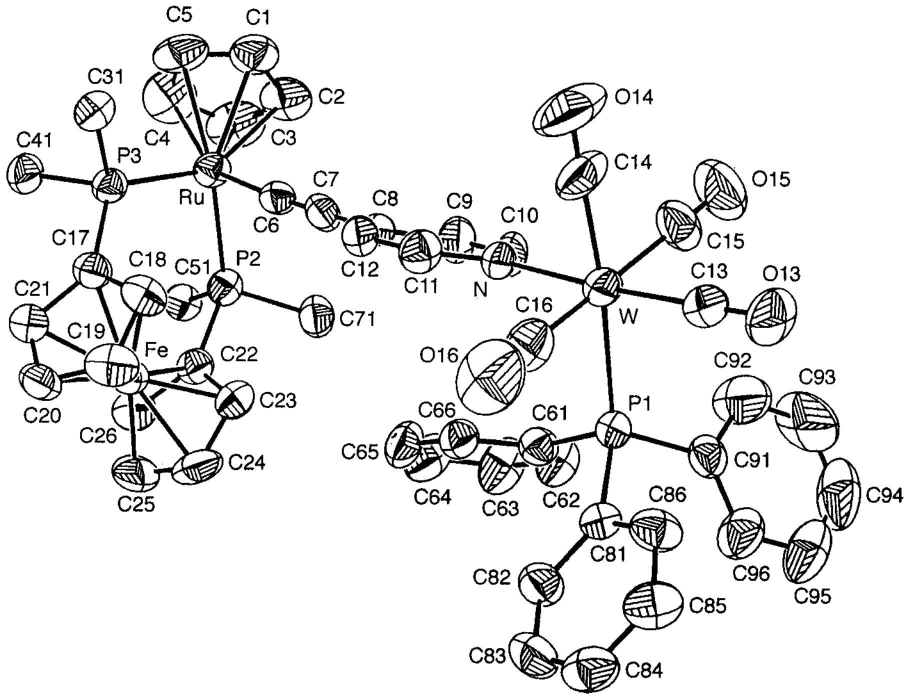

Figure 4. ORTEP drawing of complex **19**. Thermal ellipsoids are drawn with 30% probability boundaries.

broader TPA-induced fluorescence. Assuming the TPA-induced fluorescence has no substructure at 532 nm, the ratio of the TPA-induced fluorescence to the HRS signal at 532 nm can thus be obtained. From the ratio, the TPA-induced fluorescence contribution to the HRS β value is removed. After removal of the contribution from the TPA-induced fluorescence,[35] the first hyperpolarizabilities (β, 10^{-30} esu) obtained for **26**−**28** are 80, 1600, and 1400, respectively. The calculated static hyperpolarizabilities (β_0, 10^{-30} esu)[37] are 16 (**26**), 154 (**27**), and 102 (**28**) and appear to be within the values reported for analogous ruthenium acetylides reported by Humphrey.[8b] The larger optical nonlinearity of **27** and **28** compared to that of **26** is consistent with the greater conjugation length in the former. More comprehensive nonlinear optical studies on complexes in this paper and congeners are currently ongoing and will be the subject of future publications.

Molecular Structure of Ru(C≡CC$_5$H$_4$N{W(CO)$_4$-(PPh$_3$)})(η^2-dppf)(η^5-C$_5$H$_5$) (19). An ORTEP drawing of **19** is shown in Figure 4. The tungsten atom resides in an approximately octahedral environment, and the pyridyl ligand is cis to the phosphine ligand, which is similar to pyridyltungsten carbonyl structures reported by us.[9a,27c] The bite angle of dppf, P1−Ru−P2 (97.7(1)°), appears to be smaller than those (99.01(6)−101.17(7)°) of σ-acetylides of CpRu(PPh$_3$)$_2$ reported by Humphrey.[8] Humphrey suggested that the presence of a strong acceptor acetylide ligand might lengthen the Ru−P distance.[8b] However, we found that Ru−P distances for **19** (2.284(3), 2.297(3) Å), though comparable to those of Ru(C≡C(C$_6$H$_4$CH=CH)$_n$C$_6$H$_4$NO$_2$)(PPh$_3$)$_2$(η^5-C$_5$H$_5$) (n = 0, 1),° are barely longer than those in **8** (2.273(2), 2.274(2) Å).[38] The bond distances of Ru−C6 (1.99(1) Å), C6−C7 (1.21(1) Å), and C7−C8 (1.42(2) Å) appear to be normal compared to those of known ruthenium σ-acetylides.[8a]

Conclusions. We have synthesized new types of ruthenium σ-acetylides with conjugated pendant pyridine ligands. These complexes are useful precursors for construction of heterodinuclear complexes. Their pyridinium derivatives exhibit efficient charge transfer from the ruthenium donor to the organic acceptor and appear to be promising nonlinear optical materials. Further variation of conjugation bridges, such as interposition of thienyl moieties in the conjugation chain, as well as the investigation of the optical nonlinearity of new chromophores will be the subject of future study.

Appendix

After submission of our paper, a paper describing (indenyl)bis(triphenylphosphine)ruthenium acetylides with dangling terminal pyridines that were free or were attached to chromium or tungsten pentacarbonyl also appeared.[39]

Acknowledgment. We thank the Academia Sinica and the National Science Council for financial support (Grant NSC-86-2113-M-001-009).

Supporting Information Available: Tables of atomic coordinates (including hydrogen atoms), thermal parameters, and bond distances and angles for complex **19** and Figure S1, giving TPA-induced fluorescence spectra of complexes **26**−**28** (16 pages). Ordering information is given on any current masthead page.

OM9610657

(37) The β_0 value was obtained using the two-level model, with $\beta_0 = \beta[1 - (2\lambda_{max}/1064)^2][1 - (\lambda_{max}/1064)^2]$. However, it should be noted that separation of resonance enhancement contributions would require the determination of β at a different basic laser wavelength.

(38) Lo, C. M.; Lin, J. T., unpublished results.
(39) Houbrechts, S.; Clays, K.; Persoon, A.; Cadierno, V.; Gamasa, M. P.; Gimeno, J. *Organometallics* **1996**, *15*, 5266.